Impact of the first booster vaccine against SARS-CoV-2 in Chile

Emilio Molina, Diego Olguín, Antoine Brault, Paula Uribe, Pedro Gajardo, Mauricio Canals, Hector Ramirez Cabrera

Impact of the first booster vaccine against SARS-CoV-2 in Chile

Emilio Molina[a], Diego Olguín[b], Antoine Brault[c,d], Paula Uribe[c], Pedro Gajardo[e], Mauricio Canals[f], Héctor Ramírez[b,c]

[a]*INSA-Lyon, Université Claude Bernard Lyon 1, CNRS, Inserm, CREATIS UMR 5220, U1294, Villeurbanne, , France*
[b]*Departamento de Ingeniería Matemática, Universidad de Chile, Santiago, Chile*
[c]*Centro de Modelamiento Matemático, Universidad de Chile and CNRS IRL2807, Santiago, Chile*
[d]*Mathematical Modeling of Infectious Diseases Unit, Institut Pasteur, Université Paris Cité, CNRS UMR 2000, Paris, France*
[e]*Departamento de Matemática, Universidad Técnica Federico Santa María, Valparaíso, Chile*
[f]*Programa de Salud Ambiental, Escuela de Salud Pública, Facultad de Medicina, Universidad de Chile & Departamento de Medicina, Facultad de Medicina, Universidad de Chile, Santiago, Chile*

Abstract

The present paper proposes a novel methodology for evaluating the impact of a vaccination plan against a transmissible disease. The methodology has two distinct stages. The initial stage comprises a compartmental model that describes the transmission of the disease within the population. This model is composed of fundamental parts representing the vaccination status and is used in this initial stage to estimate the number of cases and deaths averted by the vaccination plan. The case dynamics generated by the compartmental model serve as the input for a data-driven model in the second part of the methodology. The second model is statistical in nature and provides additional information regarding the number of hospitalizations and ICU admissions averted. This methodology is applied to assess the impact of booster doses of the SARS-CoV-2 vaccines in Chile, resulting in an estimation of 84% (95% confidence interval (CI): 74% - 92%) of cases, 73% (95% CI: 57%, 80%) of hospital admissions, 77% (95% CI: 61%, 84%) of intensive care unit admissions, and 78% (95% CI: 62%-85%) of deaths averted between August 16 and December 31, 2021.

Keywords: SARS-CoV-2, booster vaccination, averted cases and outcomes, compartmental model, data-driven model, vaccination effectiveness.

1. Introduction

Mathematical models have been widely used in epidemiology to study the dynamics of infectious diseases, project future patterns of disease transmission, and develop and implement control strategies to prevent and mitigate outbreaks [1, 2]. However, these models may be limited by issues with parameter identification, case specificity, and robustness [1]. Mathematical models have been widely used during the COVID-19 pandemic to address specific questions, such as the rationalization of pandemic interventions and mitigation policies. The questions have changed according to the stage of the pandemic. Initially, it was crucial to determine the origin and when the outbreak started, to assess the potential for regional transmission, and to identify the risk of spread to other

locations. As the epidemic advanced, the focus shifted toward nonpharmacological interventions, disease lethality, the capacity of hospitals to accommodate patients, the effectiveness of vaccines and the estimation of avoided events. [3, 4, 5].

Many types of models have been used, such as ARIMA statistical models, machine learning and deep learning [6, 7, 8, 9], and models based on neural networks [10]. However, these types of models do not provide information regarding the transmission mechanism or its implications for disease control. Other widely used models include compartmental models, which simulate disease transmission within a population by dividing it into distinct compartments. Several variations of susceptible-exposed-infectious-removed (SEIR) compartmental models have been used to explore important features of the transmission dynamics of the COVID-19 epidemic. These include phase-based transmission [11], transmission latency [12], the role of superspreaders [13], underreporting [14], asymptomatic transmission, social distancing, quarantine, the need for hospitalization, [15, 16, 11, 17, 18, 19] and even subjective sensations such as fear of disease and perceptions of risk [20, 21].

Chile has actively employed mathematical models to address the challenges posed by COVID-19. Some examples include models for intensive care unit (ICU) admissions [22], the SEIR model for the evolution of the epidemic at the local level [4, 23], cubic polynomial adjustment and exponential adjustment to represent the daily effort to reduce the initial daily growth rate to warn about the potential of the pandemic [24], health system collapse studies [25], models of sigmoid growth [4, 26], and SIR- and SEIR-type compartmental models for the forecast of the second COVID-19 outbreak and for the study of the reliability of the parameters [27, 28].

Since the beginning of the pandemic until August 2024, Chile has reported more than 53,000 COVID-19-related deaths [29]. The initial measures implemented by the Chilean government included nonpharmaceutical interventions such as lockdowns and curfews [30]. With the emergence of vaccines against SARS-CoV-2, Chile distinguished itself by the rapidity and extensive reach of its vaccination campaign [31], as well as its early introduction of booster doses in early August 2021. This context motivated the assessment of the impact of the vaccination campaign. To perform this evaluation, in this work, we describe a novel compartmental schema to model the transmission of the SARS-CoV-2 virus, taking into account the vaccination plan. In our model, we differentiate between the various stages of vaccination, including the primary scheme and booster phase. Following the approach outlined in [11], we utilize the output of this model to estimate additional quantities not included in the compartmental model, such as hospital and ICU admissions. The objective of this study was to estimate the number of averted cases, hospital and ICU admissions, and deaths as a result of booster doses administered in Chile between August 16 and December 31, 2021. Furthermore, the methodology that we introduce can be generalized to evaluate a vaccination campaign against other transmissible diseases.

The structure of this paper is as follows. Section 2 presents the methodology employed, which includes a novel compartment model. Section 3 presents the results of the case study, namely, an evaluation of the booster vaccine against the SARS-CoV-2 virus in Chile. Section 4 presents a discussion of the results, and Section 5 presents the conclusions.

2. Methodology

This section describes the methodology employed to assess the impact of booster doses of SARS-CoV-2 vaccines on a specified population. In particular, this methodology allows for the estimation of the number of cases, deaths, hospitalizations, and ICU admissions averted as a result of the administration of booster doses.

The procedure is based on two models. The first is a compartmental model that represents the transmission of the disease in the population and is used to estimate the number of cases. The second is a statistical model that uses the number of cases to estimate the number of deaths, hospitalizations, and ICU admissions caused by SARS-CoV-2. A comprehensive description of both models is provided in the following sections.

2.1. Compartmental Model

We developed a deterministic compartmental model with homogeneous mixing, structured by vaccination status, to characterize the spread of SARS-CoV-2 in a given population. The population is divided into three fundamental groups on the basis of their vaccination status: (i) not vaccinated or partially vaccinated, (ii) fully vaccinated, and (iii) fully vaccinated with an additional booster dose. Susceptibility to infection and infectiousness upon infection depend directly on vaccination status. Furthermore, we assume that the population is isolated and constant, and we do not differentiate between the different circulating variants of the virus. This division of the population was chosen in light of the impact of vaccination on the dynamics of the disease. This is different from the existing models in the literature [11, 17].

Each fundamental group of the population is divided into 6 compartments (Figure 1): susceptible (S), asymptomatic infected (I^a), symptomatic infected (I^s), asymptomatic recovered (R^a), symptomatic recovered (R^s) and deceased (D). To distinguish variables from the three fundamental groups (Figure 1), we add the subscripts N (not vaccinated or not fully vaccinated), V (fully vaccinated) and B (vaccinated with booster). For example, the compartment denoted by S_V represents the susceptible population that received the primary vaccination schedule.

The fundamental groups are connected in a cascade structure that allows modeling of the dynamics of the disease over a time horizon in which the immunity acquired by the vaccines (primary and booster scheme) is relevant. For longer time horizons, one should consider replicating the scheme of the three fundamental units (continuing with the cascade scheme) or considering the whole population again in the first fundamental unit (unvaccinated population). The complete model, which we call the *base structure*, has 18 compartments (6 for each group), as shown in Figure 2, with the connections between the three fundamental groups corresponding to vaccination actions.

We denote the transmission rates by β_i^k for $i \in \{N, V, B\}$ and $k \in \{a, s\}$, using a for asymptomatic individuals and s for symptomatic individuals. For example, β_N^a represents the transmission rate after contact with a nonvaccinated, asymptomatic, infected person. The overall transmission rate for the susceptible group S_i with $i \in \{N, V, B\}$ is Λ_i, which is defined as:

$$\Lambda_i(t) = (1 - f_i(t)) \left(\sum_{j \in \{N,V,B\}} \beta_{i,j}^a I_j^a(t) + (1 - \mu)\beta_{i,j}^s I_j^s(t)) \right) S_i(t) \qquad i \in \{N, V, B\}. \tag{1}$$

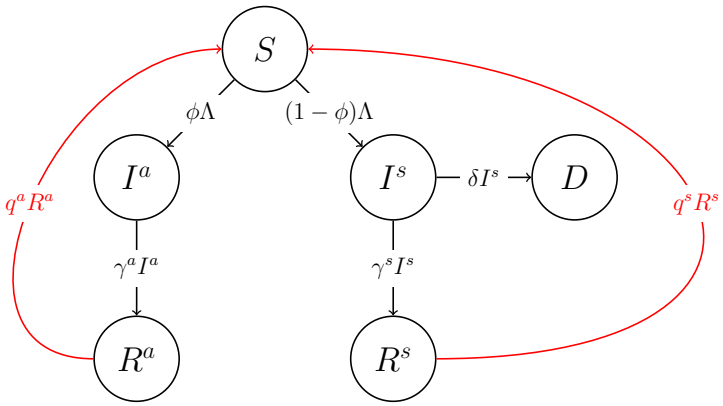

Figure 1: Flow chart of one fundamental group in the model. The population is divided into susceptible (S), asymptomatic infected (I^a), symptomatic infected (I^s), asymptomatic recovered (R^a), symptomatic recovered (R^s) and dead (D). Red arcs represent waning immunity after infection. Λ represent the transmission rates, ϕ represents the probability of being asymptomatic, γ^k represents the recovery rates, δ represents the death rates, and q^k represents the rate of waning immunity.

In equation (1), the variable $\mu \in [0,1]$ represents the proportion (assumed constant) of infected, symptomatic individuals who are completely isolated.

We denote by $f_i(t)$ the vaccine effectiveness to reduce transmission, with $f_N(t) \equiv 0$ for the non-fully vaccinated group. $e_{S_N}(\tau)$, $e_{R_N^a}(\tau)$, $e_{R_N^s}(\tau) \in [0,1]$ represents the effectiveness for the compartments (S_N), (R_N^a) and (R_N^s), respectively, τ days after fully vaccinated, and $v_{S_N}(t)$, $v_{R_N^a}(t)$ and $v_{R_N^s}(t)$ represent the vaccination rates for each compartment; then, the overall effectiveness f_i is modeled similarly to that in [17] by the following equation:

$$f_V(t) = \frac{\displaystyle\int_0^{t-t_V} \left(e_{S_N}(\tau)v_{S_N}(t-\tau) + e_{R_N^a}(\tau)v_{R_N^a}(t-\tau) + e_{R_N^s}(\tau)v_{R_N^s}(t-\tau)\right) d\tau}{\displaystyle\int_0^{t-t_V} v_{S_i}(s) + v_{R_i^a}(s) + v_{R_i^s}(s)ds} \qquad t \geq t_V, \quad (2)$$

Importantly, the effect of vaccination on recovered individuals may differ from its effect on susceptible individuals. This is the reason why different effectiveness functions are used for different compartments. The same formula is employed to compute the overall efficacy of a booster dose, represented by $f_B(t)$. Instead of using the information on fully vaccinated persons, = the booster efficacy in combination with the number of booster doses administered is used. The main innovation of this study, compared with the literature, lies in our approach to modeling the temporal evolution of vaccine effectiveness.

Finally, we describe the remaining parameters of the model:

- **Recovery rates:** We denote γ_i^k, where $i \in \{N, V, B\}$ and $k \in \{a, s\}$ are the recovery rates of infected individuals who are in the fundamental group i and could be symptomatic (s) or asymptomatic (a). A natural assumption is that recovery should be quicker for vaccinated

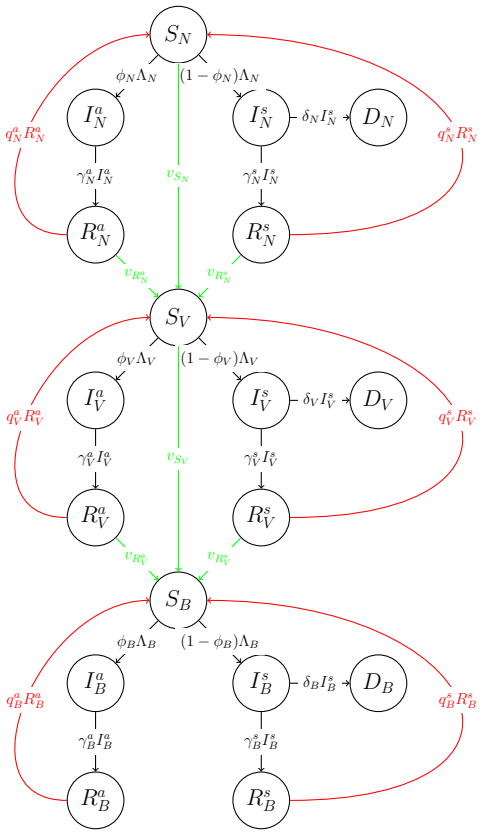

Figure 2: Base structure with 3 fundamental groups and 18 compartments in total. The population in each fundamental group is divided into susceptible (S_i), asymptomatic infected (I_i^a), symptomatic infected (I_i^s), asymptomatic recovered (R_i^a), symptomatic recovered (R_i^s) and dead (D_i) categories. The green arcs indicate vaccination actions, at the rate v_i^k, that link the three group, and the red arcs correspond to waning immunity. Λ_i represents the transmission rates, ϕ_i represents the probability of being asymptomatic, γ_i^k represents the recovery rates, δ_i represents the death rates, and q_i^k represents the rate of waning immunity for each fundamental part $i \in \{N, V, B\}$.

people (as reported, for example, in [32]), leading to the following inequalities:

$$\gamma_N^k \leq \gamma_V^k \leq \gamma_B^k \qquad k \in \{a, s\}.$$

- **Death rates:** We denote δ_i, where $i \in \{N, V, B\}$ represents the death rates in the infected population in the fundamental group i. Once again, assuming that vaccination reduces mortality (as the evidence shows in [33, 34, 35, 36]), we have the inequalities

$$\delta_B \leq \delta_V \leq \delta_N.$$

- **Rate of waning immunity:** The rate of waning immunity for a recovered individual is denoted by q_i^k, where $i \in \{N, V, B\}$ and $k \in \{a, s\}$.

- **Probability of being asymptomatic:** The probability of a susceptible individual belonging to the fundamental part $i \in \{N, V, B\}$ being asymptomatic after infection is denoted by

$\phi_i \in [0,1]$. These probabilities should fulfill

$$\phi_N \leq \phi_V \leq \phi_B,$$

because the probability of being asymptomatic should increase as vaccination advances, as shown in [37, 38, 39].

The compartmental model is defined by the following set of differential equations:

Fundamental group (N), nonvaccinated:

$$\begin{aligned}
\dot{S}_N(t) &= -\Lambda_N(t) + q_N^a R_N^a(t) + q_N^s R_N^a(t) - v_{S_N}(t) \\
\dot{I}_N^a(t) &= \phi_N \Lambda_N(t) - \gamma_N^a I_N^a(t) \\
\dot{I}_N^s(t) &= (1-\phi_N)\Lambda_N(t) - (\gamma_N^s + \delta_N) I_N^s(t) \\
\dot{R}_N^a(t) &= \gamma_N^a I_N^a(t) - q_N^a R_N^a(t) - v_{R_N^a}(t) \\
\dot{R}_N^s(t) &= \gamma_N^s I_N^s(t) - q_N^s R_N^s(t) - v_{R_N^s}(t) \\
\dot{D}_N(t) &= \delta_N I_N^s(t);
\end{aligned}$$

Fundamental group (V), vaccinated without booster:

$$\begin{aligned}
\dot{S}_V(t) &= -\Lambda_V(t) + q_V^a R_V^a(t) + q_V^s R_V^a(t) + \hat{v}_N(t) - v_{S_V}(t) \\
\dot{I}_V^a(t) &= \phi_V \Lambda_V(t) - \gamma_V^a I_V^a(t) \\
\dot{I}_V^s(t) &= (1-\phi_V)\Lambda_V(t) - (\gamma_V^s + \delta_V) I_V^s(t) \\
\dot{R}_V^a(t) &= \gamma_V^a I_V^a(t) - q_V^a R_V^a(t) - v_{R_V^a}(t) \\
\dot{R}_V^s(t) &= \gamma_V^s I_V^s(t) - q_V^s R_V^s(t) - v_{R_V^s}(t) \\
\dot{D}_V(t) &= \delta_V I_V^s(t);
\end{aligned}$$

Fundamental group (B), vaccinated with booster:

$$\begin{aligned}
\dot{S}_B(t) &= -\Lambda_B(t) + q_B^a R_B^a(t) + q_B^s R_B^a(t) + \hat{v}_V(t) \\
\dot{I}_B^a(t) &= \phi_B \Lambda_B(t) - \gamma_B^a I_B^a(t) \\
\dot{I}_B^s(t) &= (1-\phi_B)\Lambda_B(t) - (\gamma_B^s + \delta_B) I_B^s(t) \\
\dot{R}_B^a(t) &= \gamma_B^a I_B^a(t) - q_B^a R_B^a(t) \\
\dot{R}_B^s(t) &= \gamma_B^s I_B^s(t) - q_B^s R_B^s(t) \\
\dot{D}_B(t) &= \delta_B I_B^s(t).
\end{aligned}$$

2.2. Data-driven model for outcomes

We adapted a data-driven model from [11] to estimate the daily number of COVID-19-related hospital admissions, ICU admissions, and deaths from the daily number of COVID-19 cases (Figure

3). We assumed that the daily number of each outcome $O(t)$ (hospital admissions, ICU admissions or deaths) is given by a negative binomial distribution NB of mean $o(t)$ and dispersion ϕ:

$$O(t) \sim \mathrm{NB}\left(o(t), \phi\right).$$

The mean $o(t)$, which is specific to each type of outcome, is calculated on the basis of the daily number of cases $n(t)$, an exponential distribution of mean $1/\lambda$ denoted T, representing the delay between the onset of cases and the occurrence of the outcome, and the case outcome rate COR, i.e., the probability that the outcome occurs upon a case is denoted as follows:

$$o(t) = \sum_{k=0}^{t} n(k)\mathrm{COR}(k)T(t-k). \tag{3}$$

The case outcome rate $\mathrm{COR}(t)$ changes following the implementation of booster vaccination in the population, as described by the following equation:

$$\mathrm{COR}(t) = (1 - p(t))\mathrm{COR}_0 + p(t)\mathrm{COR}_0 RR,$$

where $p(t)$ is the proportion of the vaccinated population with a booster on day t, COR_0 is the case outcome rate without booster vaccination, and RR is the relative risk of an outcome occurring given that a person vaccinated with a booster is a positive COVID-19 case.

2.3. Procedure to compute averted outcomes

To calculate the number of outcomes avoided, we proceeded as follows:

1. Calibrate the parameters of the compartment, using the three fundamental groups, for the study period.
2. Calibrate the data-driven model for the study period.
3. Set $v_{S_v} = v_{R_v^a} = v_{R_v^s} = 0$ and then run the compartment model over the specified study period using the calibrated parameters. This approach guarantees that no flux is applied from the second to the third fundamental compartment; in other words, the effects of the booster dose are excluded from the simulation. The simulation provides an estimation of the number of infected individuals in the hypothetical case in which any booster dose was applied.
4. Incorporate the estimated number of infected individuals into the calibrated data-driven model to project outcomes under the scenario where no booster dose was administered, as shown in Figure 3.
5. Finally, the adverted cases are computed using the estimations from both the models and the real data.

Importantly, the calibrations of the compartment and data-driven models are completely independent, and steps 1 and 2 can be performed in parallel. The calibration of the compartment model can be performed using historic information from a subset of compartments. For example, in the study case presented in the following section, we utilize information from reported cases and

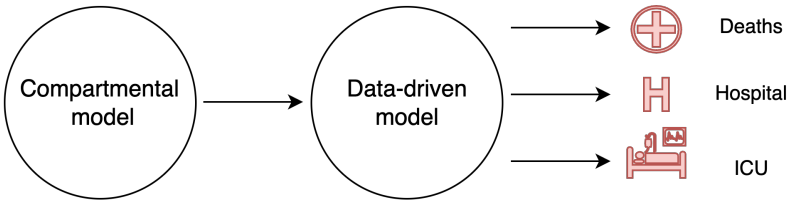

Figure 3: Representative diagram of input-output model interactions with the compartmental model.

deaths to calibrate the model. In contrast, the calibration of the data-driven model necessitates the incorporation of historical information pertaining to each estimated outcome.

This methodology allows the evaluation of different degrees of isolation of symptomatic infected people and different evolutions of vaccine effectiveness over time, including variations in the ability to transmit the virus and the probabilities of acquiring it, being symptomatic and dying.

The same methodology can be employed to assess the impact of any vaccination program against any transmissible disease. The essential aspect is to execute the compartmental model after calibration, deactivating the fundamental component associated with the vaccination state. This entails eliminating any flux within the compartment model to any compartment in this state.

3. Case Study: Averted outcomes with a COVID-19 booster dose in Chile

We apply our methodology to estimate the number of outcomes averted by the COVID-19 booster dose in Chile during the period from August 16 to December 31, 2021. The calibration was performed using the No-U-Turn Sampler (NUTS), a variant of the Markov Chain Monte Carlo (MCMC) method, implemented in Stan [40] via the Python package PyStan. The number of iterations was set to 200, and the number of warmups was set to 100.

3.1. Data description

The data used for calibration are those reported by the Chilean Ministry of Health and were downloaded from https://observa.minciencia.gob.cl/datos-abiertos/datos-del-repositorio-covid-19 (last consulted November 2024). From the onset of the pandemic until the end of the study period (December 31, 2021), the Chilean Ministry of Health reported 1,806,494 detected infections, 39,115 deaths, 46,830 ICU admissions and 169,723 hospital admissions (Figure 4).

As of September 1, 2021, approximately 13,710,836 individuals (70.4% of the Chilean population) had completed their primary vaccination scheme, and 1,616,970 individuals (8.3%) had received their booster dose. By December 31, 2021, these numbers had increased to 16,545,952 (85%) for the primary vaccination and 11,032,441 (56.5%) for the booster. Figure 5 presents the evolution of booster vaccination in the Chilean population during this period. The four main vaccines used in Chile before 2022 were CoronaVac, BNT162b2 (Pfizer), ChAdOx1 (AstraZeneca) and Ad5-nCoV (CanSino).

3.2. Compartmental model calibration

To account for fluctuations in the transmission rate over time, driven by the emergence of new variants and changes in the implementation of nonpharmaceutical interventions (e.g., lockdowns,

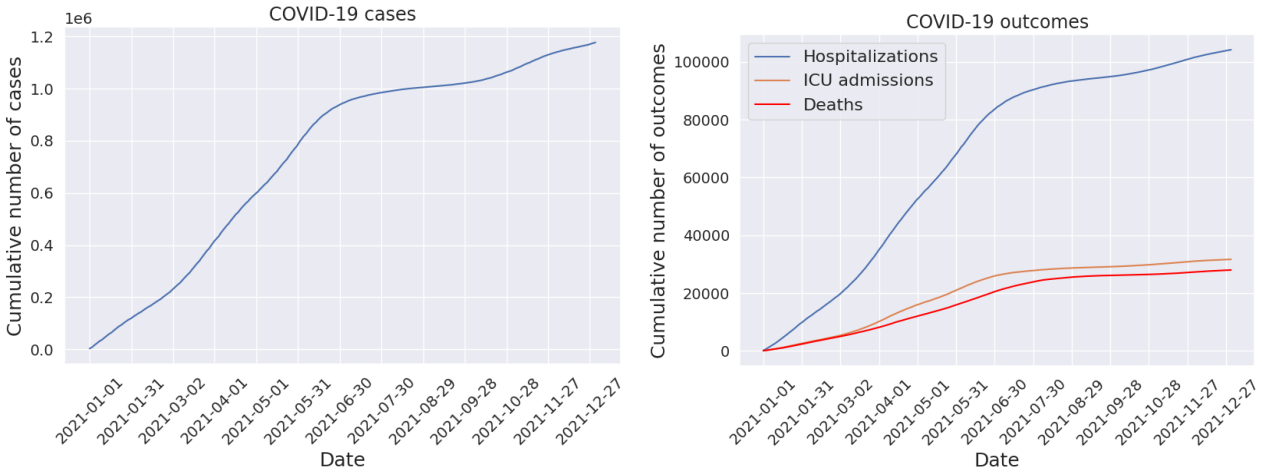

Figure 4: COVID-19 epidemic in Chile in 2021. (Left panel) Cumulative number of COVID-19 cases. (Right panel) Cumulative number of COVID-19-related hospitalizations (blue line), intensive care unit (ICU) admissions (orange line), and deaths (green line).

curfews, etc.), we divided the calibration process into five distinct periods to reflect these dynamic changes.

- The initial period is defined as the interval between December 1, 2020, and February 28, 2021. During this period, the vaccines were administered to a limited number of individuals; therefore, only the first fundamental group (N) was taken into account.

- The second period, spanning from March 1, 2021, to April 15, 2021, and the third period, spanning from April 16, 2021, to August 15, 2021, marked the commencement of a massive vaccination campaign in Chile. Consequently, during these periods, the situation is represented solely by the two initial fundamental units of the compartment model, namely, N and V. The division of the period between March 1 and August 15, 2021, into two subperiods was a response to a change in the behavior of virus transmission.

- The fourth period spans from August 16, 2021, to September 30, 2021, and the fifth period spans from October 1, 2021, to December 31, 2021. During this period, there was widespread administration of booster to the population. In terms of the compartment model, this signifies that the three fundamental units N, V and B should be considered when studying virus transmission.

Considering the aforementioned periods, the parameters utilized in the compartmental model can be classified into three distinct categories.

Constant parameters: The values of these parameters remain constant throughout the periods in which they are utilized. These values have been predetermined by the authors as a result of their modeling decisions. The parameters that fall within this category are as follows:

- The probability of being asymptomatic has been estimated in the literature with different values. On the basis of [41], we set ϕ_N equal to 0.3. Vaccination increases the proportion of

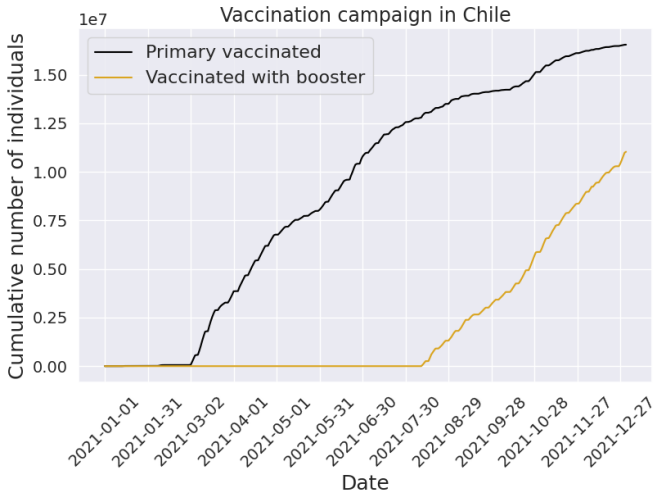

Figure 5: Vaccination campaign in Chile in 2021. Cumulative number of individuals fully vaccinated (black line), and vaccinated with a booster (yellow line).

individuals experiencing asymptomatic or mild symptoms [38]. Accordingly, we set ϕ_V and ϕ_B equal to 0.7 [42, 38].

- The proportion of symptomatic infected individuals adhering to complete isolation was fixed at $\mu = 0.7$. This parameter was selected after three possible scenarios were analyzed. The chosen value best reflected the country's actual conditions during the study period, aligning with both observed population behavior patterns and government mandates.

- The rate of waning immunity is fixed at $q_i^k = 1/480\, days^{-1}, \forall i \in \{N, V, B\}$ and $k \in \{a, s\}$ [43].

Parameters that are calibrated once: Each parameter γ_i^k and δ_i was calibrated only during its initial inclusion in the calibration procedure. For the subsequent calibration periods, these parameters were fixed at the average of those values obtained during the initial calibration.

Parameters that are calibrated each time they are used: These correspond to the transmission rates β_i^k. The parameters significantly change with respect to the prevailing strain and the government's restrictions on population interactions. Five calibration periods were used instead of three to account for the variability of this rate.

Specific consideration is given to the effectiveness of vaccines $f_i(t)$. It is evident that $f_N = 0$. For f_V and f_B, we need to know the individual efficacies $e_i(t)$. These functions are calculated on the basis of the efficacy of each vaccine at the time of their administration. On the basis of references [44, 45], we employ piecewise linear interpolation to estimate the decline in vaccine effectiveness during the pandemic, which is summarized in the left image of Figure 6. Although four vaccine brands were available in Chile during this period, namely, Pfizer, AstraZeneca, CoronaVac and CanSino, given that the CanSino vaccine was been administered to only 1% of the population, this vaccine has not been considered in our analysis, and its efficiency has been set to that of Pfizer, assuming an optimistic scenario with respect to this 1%. In our model, we use the same

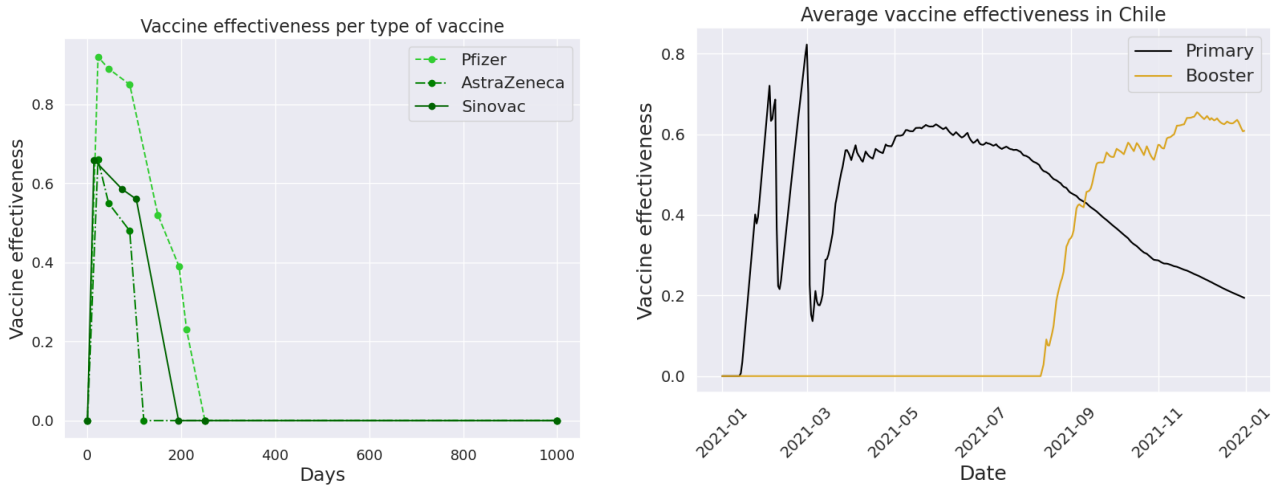

Figure 6: Vaccine effectiveness. On the left, the effectiveness over time in days $e(t)$ is shown, and on the right, the effectiveness over the transmission rate $f(t)$ is shown.

efficacies for each group and for vaccine brands . Thus, if we denote v_i and e_i, $i \in \text{Brands} = \{\text{Pfizer}, \text{AstraZeneca}, \text{CoronaVac}, \text{CanSino}\}$ (one index for each brand), the number of vaccinated and the effectiveness for the vaccine of type i, the formula (2) is reduced to formula (4).

$$f_V(t) = \frac{\displaystyle\int_0^{t-t_V} \left(\sum_{i \in Brands} e_i(\tau) v_i(t-\tau) \right) d\tau}{\displaystyle\int_0^{t-t_V} \sum_{i \in Brands} v_i(s) ds} \qquad t \geq t_V, \tag{4}$$

Assuming that the effectiveness $e_i(t)$ is the same for full vaccination and for the booster, the two curves $f_V(t)$ and $f_B(t)$ are obtained, as illustrated in the right image of Figure 6.

Importantly, the vaccination rates corresponding to the primary administration and to the booster dose in Chile are not directly observable for each group because both susceptible persons and individuals who contracted the virus and recovered were vaccinated. The rates that are observable are the vaccination rate corresponding to the complete primary scheme, which we denote $v_N(t)$, and the vaccination rate corresponding to the booster dose, which is denoted by $v_V(t)$. Therefore, it follows that:

$$v_i(t) = v_{S_i}(t) + v_{R_i^a}(t) + v_{R_i^a}(t) \quad i \in N, V$$

We further assume that the number of vaccines, either with the primary vaccination or with the booster dose, both for susceptible and recovered, is administered proportionally to the number of individuals in those compartments; then, we assume that

$$v_{\varepsilon_i}(t) = v_i(t) \left(\frac{\varepsilon_i(t)}{S_i(t) + R_i^a(t) + R_i^s(t)} \right) \quad \varepsilon_i \in \{S_i, R_i^a, R_i^s\},\ i \in N, V$$

Finally, the objective of the calibration process is to adjust the model to align with the reported curve of infected and deceased individuals by the Chilean Ministry of Health. Since this information is not disaggregated, the curves for infected and dead individuals used to fit the data are as follows:

$$I(t) = \sum_{i\in\{N,V,B\}} \sum_{k\in\{a,s\}} I_i^k(t), \quad D(t) = \sum_{i\in\{N,V,B\}} D_i(t) \tag{5}$$

Additionally, the possibility of underreporting of infected cases was considered. This underreporting represents a constant factor in the reported infected individuals and was also calibrated.

Figure 7 shows the curves $I(t)$ and $D(t)$, which were derived from the calibrations of the final two periods. These periods coincide with the application of the booster. The figure demonstrates a satisfactory alignment between the theoretical curves and the actual data.

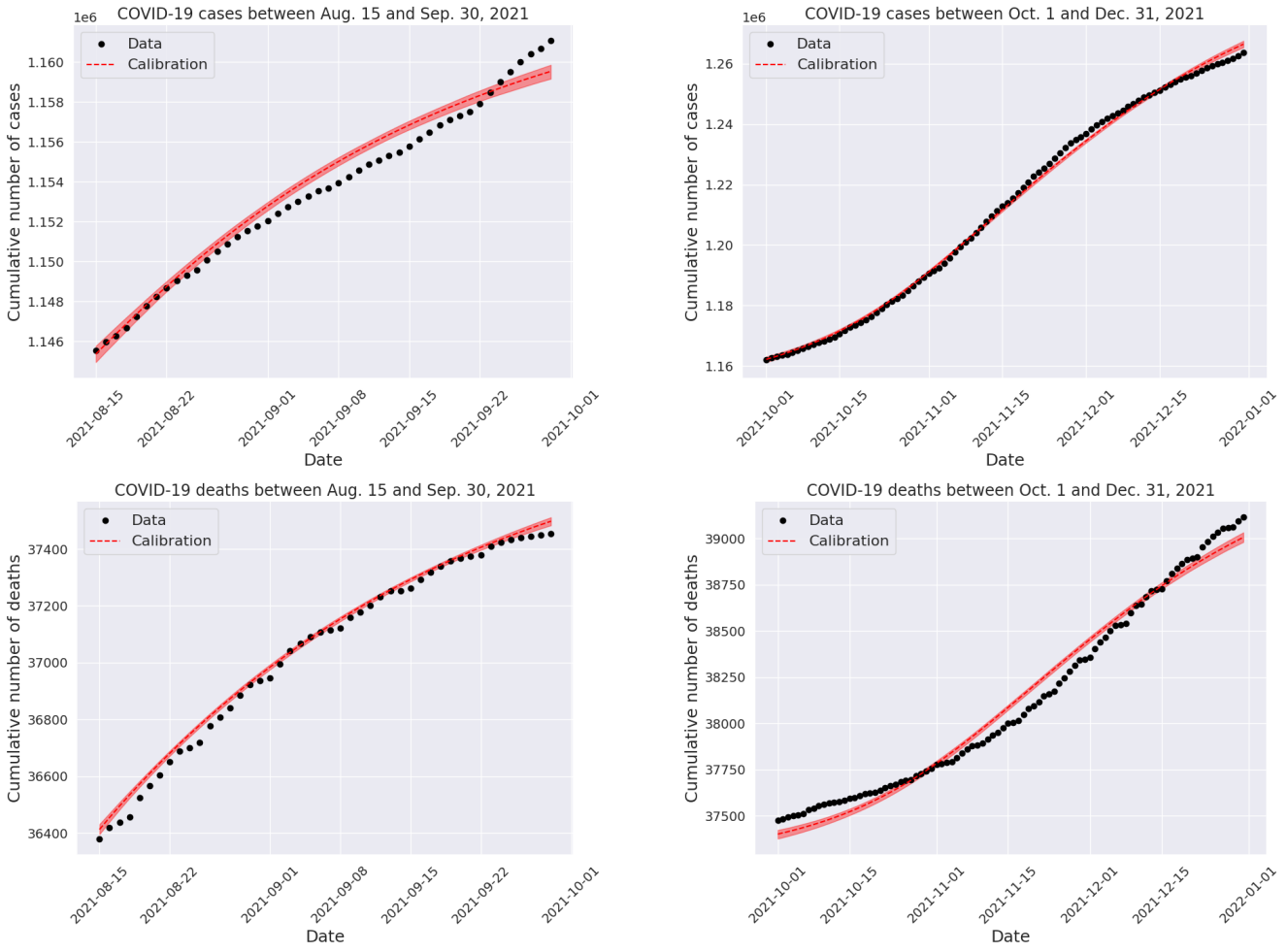

Figure 7: Case and death data (black) compared with the calibration data (red) between August 15, 2021, and December 31, 2021, divided into two periods of calibration. The images on the left represent the period between August 15, 2021, and September 30, 2021, and the images on the right represent the period between October 01, 2021, and December 31, 2021.

Notation	Description	Value	Source
β_i^k	Transmission rates	[0.45,0.95]	Fitted
μ	Proportion of symptomatic individuals who are isolated	0.7	Modeling team
$f_i(t)$	Vaccine effectiveness against transmission	Figure 6	[44, 45]
γ_i^k	Recovery rates	[0.12,0.32]	Fitted
δ_i	Death rates	[0.0013, 0.0022]	Fitted
q_i^k	Rate of waning immunity for a recovered individual	$1/480$ days^{-1}	[43]
ϕ_i	Probability of asymptomatic infection	0.3 for $i = N$ 0.7 for $i \in \{V, B\}$	[42, 41]

Table 1: Compartmental model parameters. The subscript i denotes the type of vaccination status: non-fully vaccinated (N), fully vaccinated (V), and vaccinated with booster B. The superscript k indicates whether the parameters is associated with the asymptomatic (a) or symptomatic (s) compartment. The interval represent the range of values used in simulations.

3.3. Data-driven Model Calibration

To calibrate this model, daily cases are provided by the available data . To simulate scenarios without a booster, daily cases are provided by the compartmental model. Similar to the compartmental model, the calibration was separated into two distinct periods, to be consistent with the reality of the epidemic in the Chilean population.

- The first period was between March 1, 2021, and June 30, 2021, when the booster was not yet available; thus, $p(t) = 0$ for all t in this period. Note that in this case, λ, COR_0 and ϕ are calibrated, and RR needs a period with booster vaccination. During this period, the model receives cases on all days, and the outcomes occur between April 1, 2021, and June 30, 2021; this difference in the time periods is based on the delayed effect in expression (3). The test period for the calibration was considered to be between July 1, 2021, and August 30, 2021.

- The second period was between August 16, 2021, and December 31, 2021, and the same starting point of booster vaccination was used as the compartmental model. During this period, the outcomes occurred between October 2, 2021, and December 31, 2021, again as a result of the delay effect. Given that λ, COR_0 and ϕ were estimated in the previous period, only RR was estimated.

The first period aims to fit reality in the absence of a booster, and the second aims to model a situation with booster availability. Note that these periods are not identical to those of the compartmental model. However, this is not a cause for concern, as the calibration processes are entirely independent, and the selection of the periods was based on the optimal fitting results.

For every outcome, λ and ϕ were taken with a half-normal distribution, and COR_0 was taken with a uniform distribution in $[0, 1]$. The calibrated parameters for each outcome are shown in Tables 2 and 3.

The calibration for the data-driven model in the first period, when there was no booster available, is shown in Figure 8. For this purpose, a training period, from April 1 to June 30, is given

Parameter	Hospitalization (95% CI)	ICU admissions (95% CI)	Death (95% CI)
$1/\lambda$ [days]	8.02 (5.19, 10.94)	7.71 (4.73, 10.59)	27.04 (19.37, 35.06)
COR_0	0.0898 (0.0862, 0.0932)	0.0291 (0.0278, 0.0303)	0.0246 (0.0229, 0.0266)
ϕ	29.66 (23.00, 35.92)	27.16 (21.36, 33.44)	25.17 (19.19, 31.22)

Table 2: Estimated parameters in the period without booster vaccination, with 95% confidence interval.

Outcome	Estimated RR (95% CI)
Hospitalization	1.3 (1.1, 1.5)
ICU admissions	1.9 (1.7, 2.1)
Death	2.3 (2.1, 2.5)

Table 3: Relative risk of an outcome given a positive COVID-19 case with booster vaccination, with 95% confidence interval.

for parameter calibration and then tested in the period from July 1 to September 30. Notably, the calibration results are satisfactory because the curves estimated as the means follow a trend similar to that of the observed data, and the 95% confidence interval generated effectively encapsulates the uncertainty that the data intrinsically have. This is not only observed in the training period but also in the test period, which increases the robustness of the results.

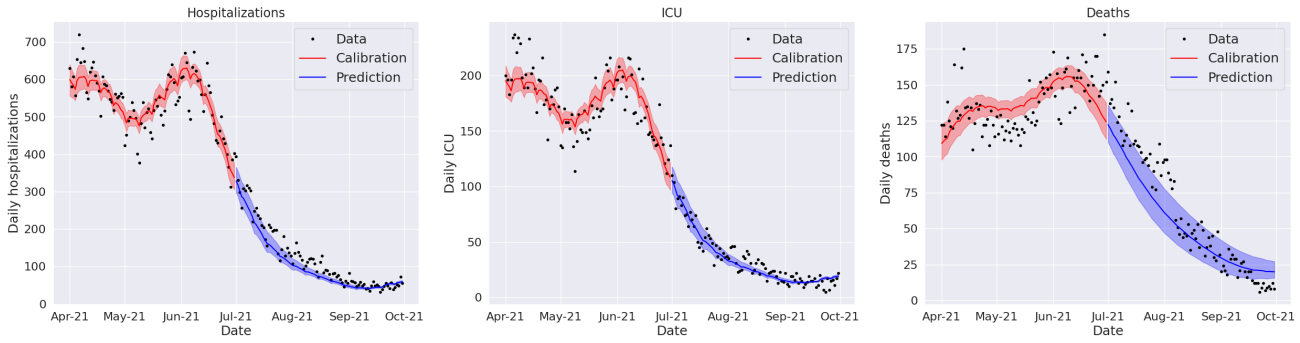

Figure 8: Data-driven model calibration for a period with no booster vaccination.

3.4. Results

To assess the impact of the booster campaign, we first estimated the number of individuals who would have been infected in the absence of the booster. This value is obtained from the compartmental model using the same parameters as those estimated during calibration and simulating a scenario without a booster, i.e., employing only the fundamental parts N and V in the compartmental model. Thus, any flow from the fundamental part V to B is eliminated. Similarly, we estimate the number of averted deaths using two approaches: directly through the compartmental model and indirectly based on case data via the data-driven model, as shown in Figure 9. The numbers of averted hospitalizations and ICU admissions were computed from the compartmental

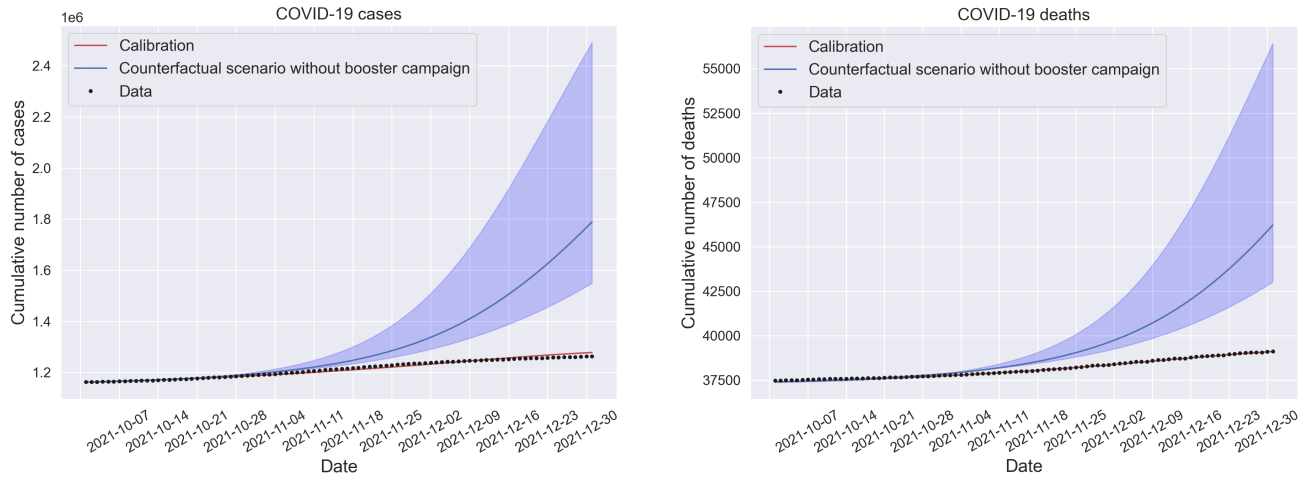

Figure 9: Compartmental model: counterfactual scenario in the absence of the COVID-19 booster campaign in Chile. Cumulative number of COVID-19 cases (left panel) and COVID-19 deaths (right panel): data (black dots), calibrated model (red line), counterfactual scenario predicted by the compartmental model (blue line).

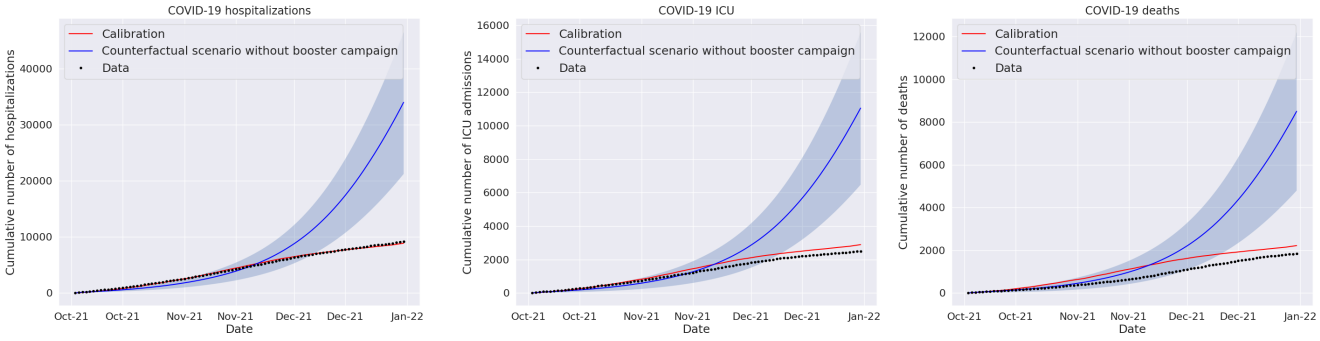

Figure 10: Data-driven model: counterfactual scenario without the COVID-19 booster campaign in Chile. Cumulative number of COVID-19 hospitalizations (left panel), COVID-19 intensive care unit admissions (middle panel) and COVID-19 deaths (right panel). The data are represented by black dots, the calibrated model by a red line, and the counterfactual scenario predicted by the data-driven model by a blue line.

model with the data-driven model (Figure 9). The curve obtained for each outcome is illustrated in Figure 10.

We define the proportion of averted outcomes with the booster campaign as follows:

$$100 \cdot \frac{\text{outcome without booster} - \text{outcomes with booster}}{\text{outcomes without booster}}\% \tag{6}$$

The number of cases averted are shown in Table 4. Notably, the results demonstrate a significant reduction in both the infected and deceased cases, with an 80 % decrease attributed to the booster campaign. Furthermore, the estimated number of deaths in each model is notably similar, indicating a high degree of consistency in the results.

Model	Outcome	Averted percentage (CI 95%)	Averted quantity (CI 95%)
Compartmental	Cases	84% (74 % - 92 %)	525476 (285453 - 1227928)
	Deaths	81 % (70 % - 91 %)	7097 (3895 - 17312)
Data-driven	Hospitalizations	73% (57%, 80%)	24813 (12098, 37466)
	ICU admissions	77% (61%, 84%)	8573 (3983, 13129)
	Deaths	78% (62%, 85%)	6686 (2961, 10400)

Table 4: The table show the percentage and quantity of cases averted as a result of the booster campaign as estimated using the compartmental model.

4. Discussion

During the initial phase of the COVID-19 pandemic, many countries implemented mass vaccination campaigns, often complemented by nonpharmaceutical interventions (NPIs). In the European Union, two main strategies emerged. The first involves the rapid increase in NPIs, which rely on natural exposure and vaccination to achieve herd immunity, maintain a manageable incidence rate and avoid overwhelming health care systems. The second strategy focused on gradually easing restrictions in parallel with vaccination progress, aiming to keep incidence rates low while supporting efforts with an efficient test-trace-isolate program.

In 2021, Chile adopted an approach closer to the first strategy, emphasizing mass vaccination with rapid and extensive coverage [46]. The vaccination campaign began with health care personnel and high-risk groups in December 2020, followed by the launch of mass vaccination for the general population on February 3, 2021. During the analyzed period, the campaign utilized four main vaccines: CoronaVac (Sinovac Life Sciences, 60.9%), BNT162b2 (Pfizer-BioNTech, 29.6%), ChAdOx1-S (AstraZeneca, 7.9%), and Recombinant Ad5.nCoV (CanSino Biologics Inc., 1.5%). These vaccines exhibited varying levels of effectiveness against symptomatic cases, hospitalizations, ICU admissions, and COVID-19-related deaths. For example, Jara et al. [44] reported that, among individuals with complete vaccination series, vaccine effectiveness was 65.9% (95% CI: 65.2%-66.6%) for preventing COVID-19, 87.5% (95% CI: 86.7%-88.2%) for preventing hospitalization, 90.3% (95% CI: 89.1%-91.4%) for preventing ICU admission, and 86.3% (95% CI: 84.5%-87.9%) for preventing COVID-19-related deaths.

To better understand and quantify the impact of these vaccination efforts, we developed a new model for the spread of infectious diseases. Our model incorporates both primary vaccination and booster doses, as well as the evolution of vaccine efficacy over time. Coupled with a statistical framework that uses case numbers as input, this model estimates hospitalizations, ICU admissions, and deaths, enabling us to quantify the number of these outcomes prevented due to vaccination boosters.

We based our work on the model proposed by Giordano et al. (2021) [11], adapting it to include critical factors such as booster administration and the time-dependent decline in vaccine efficacy. This approach is particularly relevant to the vaccination context in Chile, where the COVID-19 vaccination campaign employed a diverse range of vaccines with varying durations of protection. Unlike existing studies [4, 23, 24, 25, 47, 48], our model accounts for the population's average vaccine effectiveness, which is dynamically determined by the efficacy trajectory following each dose and the distribution of vaccines administered within the population.

Our findings can be compared with those reported by Brault et al. (2024) [5]. In their study, 148,268 COVID-19 cases were estimated to have been avoided during the period analyzed (until December 31, 2021). In contrast, our compartmental model estimates that a significantly greater number of cases was prevented - 525,476 (CI 285,453–1227,928). This discrepancy may be explained by differences in methodology; while Brault et al. rely on differences in observed incidence rates, our model explicitly incorporates vaccine impact on transmission dynamics. However, there is notable agreement between the two studies in terms of the number of deaths averted. Brault et al. estimated that 7,990 deaths were prevented by booster doses in the same period, a figure that is consistent with our model's predictions.

There are limitations in our study. Our model is a compartmental type that is based on the assumption of a large population with a homogeneous mixture and provides predictions that are averaged over the entire population; therefore, spatial heterogeneity is not taken into account. We did not consider some possible confounding variables, such as comorbidities, socioeconomic strata, testing rates, etc. On the other hand, nonpharmacological interventions, such as the use of masks, mobility passes, social distancing, remote work and other measures whose influence on different outcomes cannot be quantified, were also carried out during the vaccination campaign. Furthermore, it is assumed that vaccines are effective regardless of the dominant variant, among which, in 2021 in Chile, the γ variant (P.1), the Andean variant (λ; C.12) and the δ variant were predominant. In this context, it has been proposed that some variants may escape vaccine-induced immunity [49, 50], affecting the risk of reinfection by SARS-CoV-2 [51]. These limitations, however, are common to the vast majority of compartment models [3].

5. Conclusion

Given that vaccines and variants impact the transmission dynamics of SARS-CoV-2, the development of new models is crucial for forecasting epidemic scenarios and evaluating the impact of implemented interventions. The methodology proposed in this paper demonstrates potential broad applicability beyond the present case study, offering a robust framework for evaluating pharmacological interventions in future pandemic scenarios. This approach provides a systematic method for assessing therapeutic effectiveness in rapidly evolving public health emergencies while being adaptable to the dynamics of various infectious diseases. The framework encompasses multiple critical variables, including multistage vaccination schemes, symptom manifestations, and various severity outcomes, such as hospitalization, intensive care unit admission, and mortality. This comprehensive approach enables rigorous evaluation of intervention effectiveness across different epidemiological contexts.

6. Acknowledgments

This work was supported by the Center for Mathematical Modeling (CMM) BASAL FB210005 for Center of Excellence from ANID-Chile, PAHO/WHO Project CON21-00013967 Impact of the COVID-19 Vaccination Campaign and Modeling of SARS-CoV-2 Immunization Strategy Scenarios in Chile for Decision-Making Support, Joint Cooperation Fund Chile-Mexico 2022: 'Mathematical Modeling of Epidemic Processes, Incorporating Population Structure, Regional Distribution and Risk Groups'. Antoine Brault was funded by ANID postdoctoral fellowship 3200116.

References

[1] G. Chowell, Fitting dynamic models to epidemic outbreaks with quantified uncertainty: A primer for parameter uncertainty, identifiability, and forecasts, Infect. Dis. Model. 2 (3) (2017) 379–398.

[2] M. Masum, M. A. Masud, M. I. Adnan, H. Shahriar, S. Kim, Comparative study of a mathematical epidemic model, statistical modeling, and deep learning for COVID-19 forecasting and management, Socioecon. Plann. Sci. 80 (101249) (2022) 101249.

[3] A. Adiga, D. Dubhashi, B. Lewis, M. Marathe, S. Venkatramanan, A. Vullikanti, Models for COVID-19 pandemic: A comparative analysis (Sep. 2020). arXiv:2009.10014.

[4] M. Canals, C. Cuadrado, A. Canals, COVID-19 in chile: The usefulness of simple epidemic models in practice, Medwave 21 (1) (2021) e8119.

[5] A. Brault, A. Hart, P. Uribe, J. Prado, J. San Martín, A. Maass, M. Canals, Direct impact of COVID-19 vaccination in chile: averted cases, hospitalizations, ICU admissions, and deaths, BMC Infect. Dis. 24 (1) (2024) 467.

[6] H. Tandon, P. Ranjan, T. Chakraborty, V. Suhag, Coronavirus (COVID-19): ARIMA-based time-series analysis to forecast near future and the effect of school reopening in india, J. Health Manag. 24 (3) (2022) 373–388.

[7] F. Petropoulos, S. Makridakis, Forecasting the novel coronavirus COVID-19, PLoS One 15 (3) (2020) e0231236.

[8] M. H. D. M. Ribeiro, R. G. da Silva, V. C. Mariani, L. D. S. Coelho, Short-term forecasting COVID-19 cumulative confirmed cases: Perspectives for brazil, Chaos Solitons Fractals 135 (109853) (2020) 109853.

[9] M. Maleki, M. R. Mahmoudi, D. Wraith, K.-H. Pho, Time series modelling to forecast the confirmed and recovered cases of COVID-19, Travel Med. Infect. Dis. 37 (101742) (2020) 101742.

[10] G. R. Shinde, A. B. Kalamkar, P. N. Mahalle, N. Dey, J. Chaki, A. E. Hassanien, Forecasting models for coronavirus disease (COVID-19): A survey of the state-of-the-art, SN Comput. Sci. 1 (4) (Jul. 2020).

[11] G. Giordano, M. Colaneri, A. Di Filippo, F. Blanchini, P. Bolzern, G. De Nicolao, P. Sacchi, P. Colaneri, R. Bruno, Modeling vaccination rollouts, sars-cov-2 variants and the requirement for non-pharmaceutical interventions in italy, Nature medicine 27 (6) (2021) 993–998.

[12] Z. Liu, P. Magal, O. Seydi, G. Webb, A COVID-19 epidemic model with latency period, Infect. Dis. Model. 5 (2020) 323–337.

[13] C. Y. Yang, J. Wang, A mathematical model for the novel coronavirus epidemic in wuhan, china, Math. Biosci. Eng. 17 (3) (2020) 2708–2724.

[14] M. Serhani, H. Labbardi, Mathematical modeling of COVID-19 spreading with asymptomatic infected and interacting peoples, J. Appl. Math. Comput. 66 (1-2) (2021) 1–20.

[15] S. E. Eikenberry, M. Mancuso, E. Iboi, T. Phan, K. Eikenberry, Y. Kuang, E. Kostelich, A. B. Gumel, To mask or not to mask: Modeling the potential for face mask use by the general public to curtail the covid-19 pandemic, Infectious disease modelling 5 (2020) 293–308.

[16] K. Leung, J. T. Wu, D. Liu, G. M. Leung, First-wave covid-19 transmissibility and severity in china outside hubei after control measures, and second-wave scenario planning: a modelling impact assessment, The Lancet 395 (10233) (2020) 1382–1393.

[17] A. Ramos, M. Vela-Pérez, M. Ferrández, A. Kubik, B. Ivorra, Modeling the impact of SARS-CoV-2 variants and vaccines on the spread of COVID-19, Communications in Nonlinear Science and Numerical Simulation 102 (2021) 105937. doi:https://doi.org/10.1016/j.cnsns.2021.105937.
URL https://www.sciencedirect.com/science/article/pii/S1007570421002495

[18] D. W. Berger, K. F. Herkenhoff, S. Mongey, An seir infectious disease model with testing and conditional quarantine, Tech. rep., National Bureau of Economic Research (2020).

[19] J. F. Oliveira, D. C. Jorge, R. V. Veiga, M. S. Rodrigues, M. F. Torquato, N. B. da Silva, R. L. Fiaccone, L. L. Cardim, F. A. Pereira, C. P. de Castro, et al., Mathematical modeling of covid-19 in 14.8 million individuals in bahia, brazil, Nature communications 12 (1) (2021) 333.

[20] M. D. Johnston, B. Pell, A dynamical framework for modeling fear of infection and frustration with social distancing in COVID-19 spread, Math. Biosci. Eng. 17 (6) (2020) 7892–7915.

[21] T. Usherwood, Z. LaJoie, V. Srivastava, A model and predictions for COVID-19 considering population behavior and vaccination, Sci. Rep. 11 (1) (2021) 12051.

[22] R. I. Gonzalez, F. Munoz, P. S. Moya, M. Kiwi, Is a COVID19 quarantine justified in chile or USA right now? (2020).

[23] C. Guerrero-Nancuante, R. Manríquez P, An epidemiological forecast of COVID-19 in chile based on the generalized SEIR model and the concept of recovered, Medwave 20 (4) (2020) e7898.

[24] F. Córdova-Lepe, R. Gutiérrez-Aguilar, J. P. Gutiérrez-Jara, Number of COVID-19 cases in chile at 120 days with data at 21/03/2020 and threshold of daily effort to flatten the epi-curve, Medwave 20 (2) (2020) e7861.

[25] R. Gutiérrez-Aguilar, F. Córdova-Lepe, M. T. Muñoz-Quezada, J. P. Gutiérrez-Jara, Model for a threshold of daily rate reduction of COVID-19 cases to avoid hospital collapse in chile, Medwave 20 (3) (2020) e7871.

[26] F. Novoa-Muñoz, Models to predict the number of infected cases and deaths from COVID-19 in chile and its most affected regions, Discrete Dyn. Nat. Soc. 2022 (1) (2022) 1–13.

[27] P. Cumsille, Ó. Rojas-Díaz, P. M. de Espanés, P. Verdugo-Hernández, Forecasting COVID-19 chile' second outbreak by a generalized SIR model with constant time delays and a fitted positivity rate, Math. Comput. Simul. 193 (2022) 1–18.

[28] R. Bürger, G. Chowell, I. Kröker, L. Y. Lara-Díaz, A computational approach to identifiability analysis for a model of the propagation and control of COVID-19 in chile, J. Biol. Dyn. 17 (1) (2023) 2256774.

[29] Cifras oficiales. gobierno de chile., `https://www.gob.cl/pasoapaso/cifrasoficiales/#datos`, accessed: 2024-09-10.

[30] Paso a paso - gob.cl. gobierno de chile., `https://www.gob.cl/pasoapaso/`, accessed: 2024-09-10.

[31] A. Shepherd, Covid-19: Chile joins top five countries in world vaccination league (2021).

[32] P. Maclean, A. Mentzer, T. Lambe, J. Knight, Why do breakthrough covid-19 infections occur in the vaccinated?, QJM: An International Journal of Medicine 115 (2) (2022) 67–68.

[33] R. Arbel, R. Sergienko, M. Friger, A. Peretz, T. Beckenstein, S. Yaron, D. Netzer, A. Hammerman, Effectiveness of a second bnt162b2 booster vaccine against hospitalization and death from covid-19 in adults aged over 60 years, Nature medicine (2022) 1–5.

[34] G. Lv, J. Yuan, X. Xiong, M. Li, Mortality rate and characteristics of deaths following covid-19 vaccination, Frontiers in Medicine (2021) 649.

[35] J. Kennedy, Vaccine hesitancy: a growing concern, Pediatric drugs 22 (2) (2020) 105–111.

[36] A. Roghani, et al., The influence of covid-19 vaccination on daily cases, hospitalization, and death rate in tennessee, united states: Case study, JMIRx med 2 (3) (2021) e29324.

[37] M. Aguiar, J. Van-Dierdonck, J. Mar, N. Stollenwerk, The role of mild and asymptomatic infections on covid-19 vaccines performance: a modeling study, Journal of Advanced Research 39 (2022) 157–166.

[38] F. Chirico, G. Nucera, O. Ilesanmi, A. Afolabi, M. Pruc, L. Szarpak, Identifying asymptomatic cases during the mass covid-19 vaccination campaign: insights and implications for policy makers (2022).

[39] L. Tang, D. Hijano, A. Gaur, T. Geiger, E. Neufeld, J. Hoffman, R. Hayden, Asymptomatic and symptomatic sars-cov-2 infections after bnt162b2 vaccination in a routinely screened workforce, Jama 325 (24) (2021) 2500–2502.

[40] B. Carpenter, A. Gelman, M. D. Hoffman, D. Lee, B. Goodrich, M. Betancourt, M. Brubaker, J. Guo, P. Li, A. Riddell, Stan: A probabilistic programming language, Journal of Statistical Software 76 (1) (2017) 1–32. doi:10.18637/jss.v076.i01.
URL https://www.jstatsoft.org/index.php/jss/article/view/v076i01

[41] D. P. Oran, E. J. Topol, Prevalence of asymptomatic sars-cov-2 infection: a narrative review, Annals of internal medicine 173 (5) (2020) 362–367.

[42] M. Al-Qahtani, S. AlAli, A. AbdulRahman, A. S. Alsayyad, S. Otoom, S. L. Atkin, The prevalence of asymptomatic and symptomatic covid-19 in a cohort of quarantined subjects, International journal of infectious diseases 102 (2021) 285–288.

[43] J. P. Townsend, H. B. Hassler, Z. Wang, S. Miura, J. Singh, S. Kumar, N. H. Ruddle, A. P. Galvani, A. Dornburg, The durability of immunity against reinfection by sars-cov-2: a comparative evolutionary study, The Lancet Microbe 2 (12) (2021) e666–e675.

[44] A. Jara, E. A. Undurraga, C. González, F. Paredes, T. Fontecilla, G. Jara, A. Pizarro, J. Acevedo, K. Leo, F. Leon, C. Sans, P. Leighton, P. Suárez, H. García-Escorza, R. Araos, Effectiveness of an inactivated SARS-CoV-2 vaccine in chile, N. Engl. J. Med. 385 (10) (2021) 875–884.

[45] P. Nordström, M. Ballin, A. Nordström, Effectiveness of covid-19 vaccination against risk of symptomatic infection, hospitalization, and death up to 9 months: a swedish total-population cohort study, Hospitalization, and Death Up to 9 (2021).

[46] M. Canals, A. Canals, Resumen analítico de la experiencia chilena de la pandemia COVID-19, 2020-2022, Cuad. Med. Soc. 62 (3) (2022) 5–16.

[47] N. Ferguson, D. Laydon, G. Nedjati Gilani, N. Imai, K. Ainslie, M. Baguelin, S. Bhatia, A. Boonyasiri, Z. Cucunuba Perez, G. Cuomo-Dannenburg, A. Dighe, I. Dorigatti, H. Fu, K. Gaythorpe, W. Green, A. Hamlet, W. Hinsley, L. Okell, S. Van Elsland, H. Thompson, R. Verity, E. Volz, H. Wang, Y. Wang, P. Walker, P. Winskill, C. Whittaker, C. Donnelly, S. Riley, A. Ghani, Report 9: Impact of non-pharmaceutical interventions (NPIs) to reduce COVID19 mortality and healthcare demand, Tech. rep., Imperial College London (2020).

[48] C. Castillo-Laborde, T. de Wolff, P. Gajardo, R. Lecaros, G. Olivar-Tost, H. Ramírez C, Assessment of event-triggered policies of nonpharmaceutical interventions based on epidemiological indicators, J. Math. Biol. 83 (4) (2021) 42.

[49] S. M. Hirabara, T. D. A. Serdan, R. Gorjao, L. N. Masi, T. C. Pithon-Curi, D. T. Covas, R. Curi, E. L. Durigon, SARS-COV-2 variants: Differences and potential of immune evasion, Front. Cell. Infect. Microbiol. 11 (2021) 781429.

[50] J. Angulo, C. Martinez-Valdebenito, C. Pardo-Roa, L. I. Almonacid, E. Fuentes-Luppichini, A. M. Contreras, C. Maldonado, N. Le Corre, F. Melo, R. A. Medina, M. Ferrés, Assessment of mutations associated with genomic variants of SARS-CoV-2: RT-qPCR as a rapid and

affordable tool to monitoring known circulating variants in chile, 2021, Front. Med. (Lausanne) 9 (2022) 841073.

[51] P. Nordström, M. Ballin, A. Nordström, Risk of SARS-CoV-2 reinfection and COVID-19 hospitalisation in individuals with natural and hybrid immunity: a retrospective, total population cohort study in sweden, Lancet Infect. Dis. 22 (6) (2022) 781–790.